INSTITUTE FOR NUCLEAR STUDY
UNIVERSITY OF TOKYO
Tanashi, Tokyo 188
Japan

INS-Rep.-1049
Aug. 1994

INS--1049

JP9501214

New Algorithm for Hartree-Fock Variational Equation

K. Iwasawa[a], F. Sakata[a], Y. Hashimoto[b] and J. Terasaki[a]

[a] Institute for Nuclear Study, University of Tokyo, Tanashi, Tokyo 188, Japan
[b] Institute of Physics, University of Tsukuba, Ibaraki 305, Japan

Contents

1 Introduction

According to the recent development of the nuclear structure physics, a semi-quantum treatment within the mean-field theory, *e.g.*, the rotating shell model, has played a decisive role in understanding complex structure of various nuclear excited states. In these studies, it becomes clear that there often coexist many stable mean-fields with different deformation within one nucleus[1]. Before developing a full-quantum theory capable of describing the collective excited states situated far away from the ground state, therefore, it is desirable to develop the semi-quantum theory of the large-amplitude collective motions which are influenced by many local minima with different deformations. In this case, one is involved into many theoretical subjects[2] related to the *adiabatic* and *diabatic* single-particle states, the *adiabatic* and *diabatic* collective potentials, the *level crossing* of single-particle orbitals, the configuration change in the ground state, a relation between various stable mean-fields which are not necessarily orthogonal with each other, *etc.*

Exploring the above basic theoretical problems, one has to start with discussing how to obtain many Hartree-Fock (HF) states for a given nuclear Hamiltonian. In the conventional algorithm of solving the constrained (C-)HF equation, which has been emploied in obtaining the many HF-points, an *adiabatic* assumption is frequently required. However, the above mentioned problems are known to be essentially related to this adiabatic approximation. As was pointed out in Ref.[1, 3], moreover, the adiabatic (A-)CHF method (or its approximation through the Nilsson-Strutinsky method) often gives a shallow second HF-minimum or only a small shoulder, rather than a well developed second local minimum which is expected from the experimental data. On the other hand, one has been used to numerically solve the HF equation by imposing an orthogonality condition to the HF ground state, for obtaining excited HF states. Since this method often ignores many local minima through an additional kinematical constraint, the complex structure of the time-dependent (TD-)HF manifold can not be studied by using this method.

In order to develop a fairly general numerical method capable of reaching many HF points in the TDHF-manifold, in the previous paper [4], we elucidated the CHF method within a simple schematic model. It was clarified that the solutions of the CHF equation gives *differentiable* lines within the TDHF-coordinate space, and each HF-point rests on one of these lines. It was also pointed out that the configuration change occurs smoothly along the differentiable CHF-line, without any abrupt rearrangement of the single-particle configuration. In other words, discontinuous configuration change will take place when one jumps over from one differentiable CHF-line to the other. By fully exploiting a differentiable nature of the CHF-lines in the TDHF-coordinate space, in the present paper, we develop a new algorithm for obtaining the many HF-points as well as the many continuous CHF-lines in the realistic nuclear system. An introduction of many HF points not necessarily orthogonal with one another requires the full analysis of the gauge structure of the TDHF-manifold,

which will be discussed in the separated paper[5].

Here, the pairing correlation is known to affect on the configuration change considerably in the actual nuclei. In order to study many-body dynamics near the level-crossing region, the dynamical effects of various correlations on the configuration change should be explored separately. In this paper, therefore, we restrict ourselves to the configuration change due to the particle-hole correlations. The effects coming from the pairing correlations will be discussed within the the TDHF-Bogoliubov manifold in the forthcoming paper.

In Sec. 2, we describe the basic concept of our method. The algorithm is explained in Sec. 3 together with the numerical results with Skyrme force. Section 4 is devoted to the summary and discussion.

2 Differentiability of Constrained Hartree-Fock Solution

2.1 Time-Dependent Hartree-Fock Coordinate Space

The CHF equation is expressed as

$$\delta\langle\phi|\hat{H} - \lambda\hat{Q}|\phi\rangle = 0, \tag{2.1}$$

$$\langle\phi|\hat{Q}|\phi\rangle = q, \tag{2.2}$$

where $\hat{Q}$ denotes a constraining operator put in by hand. Since one usually introduces a small number of constraining operators, a *constraining coordinate system* $\{q\}$ defined by the expectation values of $\hat{Q}$'s does not uniquely specify the single Slater-determinant. However, the small dimensionality of the $\{q\}$-space makes it feasible to numerically solve Eqs.(2.1) and (2.2) by either the gradient method [6] or an iterative diagonalization method so as to obtain the *most energetically favorable* single Slater-determinant satisfying a given constrained condition. (In this paper, these methods will be called the ACHF.)

On the other hand, one may introduce the *TDHF-coordinate system* $\{x_{\mu i}\}$, which can uniquely specify the time-*in*dependent single Slater-determinant. Here $\{x_{\mu i}\}$ is introduced as follows: Suppose there exists a certain HF state $|\phi_0\rangle$. By means of the particle- and hole-creation operators $\hat{a}^\dagger_\mu$ and $\hat{b}^\dagger_i$ with respect to $|\phi_0\rangle$, the general time-dependent single Slater-determinant $|\phi\rangle$ is expressed as

$$|\phi\rangle \equiv e^{\hat{F}}|\phi_0\rangle, \quad \hat{F} \equiv \sum_{\mu i}(f_{\mu i}\hat{a}^\dagger_\mu\hat{b}^\dagger_i - h.c.). \tag{2.3}$$

With the aid of particle-hole amplitudes $f_{\mu i}$, the TDHF (symplectic) manifold $\mathcal{M}$: $\{p_{\mu i}, x_{\mu i}\}$ is defined as

$$p_{\mu i} \equiv \frac{i}{\sqrt{2}}(C_{\mu i} - C^*_{\mu i}), \quad x_{\mu i} \equiv \frac{1}{\sqrt{2}}(C_{\mu i} + C^*_{\mu i}),$$
$$C_{\mu i} \equiv (f\frac{\sin\sqrt{f^\dagger f}}{\sqrt{f^\dagger f}})_{\mu i}, \quad C^*_{\mu i} \equiv (\frac{\sin\sqrt{f^\dagger f}}{\sqrt{f^\dagger f}}f^\dagger)_{i\mu}. \tag{2.4}$$

In this paper we only consider the TDHF-coordinate space $\{x_{\mu i}\}$, because we are interested in the stationary points of the potential energy surface (PES) within the TDHF-manifold.

The solution of the CHF equation within the $\{x_{\mu i}\}$-space was studied in the previous paper[4]. It was shown that the first equation of the CHF method in Eq.(2.1) defines differentiable lines within the $\{x_{\mu i}\}$-space, which do not cross with one another. It also gives a concrete value of the Lagrange multiplier λ at each point on these lines. Every HF point rests on one of these lines, which will be called *CHF-lines* within the $\{x_{\mu i}\}$-space. By expressing the expectation value of the constraining operator as a function of $x_{\mu i}$, on the other hand, the second equation of the CHF method in Eq.(2.2) defines a transformation from the TDHF-coordinate space to the constraining coordinate space:

$$\{x_{\mu i}\} \rightarrow \{q\} : q = Q(x_{\mu i}), \ (= \langle\phi|\hat{Q}|\phi\rangle). \tag{2.5}$$

Here it should be noticed that Eq.(2.5) gives a smooth many-to-one transformation and $q = Q(x_{\mu i})$ is a differentiable function of $x_{\mu i}$.

With the aid of Eq.(2.5), the potential energy on many differentiable lines in the $\{x_{\mu i}\}$-space is transformed to that in the $\{q\}$-space. Here it should be noted that two points located far away with each other in the $\{x_{\mu i}\}$-space are often transformed to the almost same point in the $\{q\}$-space. Therefore, the CHF equation in the $\{q\}$-space has many solutions (many single Slater-determinants) satisfying Eq.(2.1) for a given constrained condition (2.2). The ACHF is then regarded as a practical method to avoid the above stated multi-valuedness. When one applies the adiabatic requirement, however, one often overlooks and eventually disregards many well-developed HF-points which are lying above the adiabatic PES. Moreover, the adiabatic requirement meets some difficulty in the *band crossing region* where two CHF solutions satisfying the same constrained condition have accidental degeneracy[7].

Since the CHF equation gives differentiable lines in the $\{x_{\mu i}\}$-space, and the $q = Q(x_{\mu i})$ is a differentiable function of $x_{\mu i}$, the CHF equation in the $\{q\}$-space also gives smooth continuous lines, which is also called the CHF-lines in the $\{q\}$-space. This means that there does not occur any sudden change in the configuration of the single Slater-determinants, when they are lying on the single CHF-line in the $\{q\}$-space with sufficiently small distance. Therefore, many diabatic recipes[8, 9, 10, 11] are understood to be a phenomenological method which effectively simulate the continuous property of the CHF-lines.

Since every HF-point satisfies the CHF condition, it is desirable to exploit a continuous property of the CHF-lines in the $\{q\}$-space in obtaining many HF-points, rather than to use the adiabatic requirement. Namely, one may use the CHF-lines as a searching path to reach the high-lying HF states.

2.2 Continuity Condition for Single Slater-Determinant

In the conventional ACHF calculation for the N-particle system, each iterative process is achieved by introducing a new density matrix constructed by the first N-lowest eigenvectors of the one-body Hamiltonian (adiabatic assumption), which is defined by using the preceding density matrix. The convergence process is completed when the resultant density matrix becomes equivalent to the preceding density matrix. In this numerical method, one does not pay any attention to mutual relations between two neighboring Slater-determinants with slightly different constrained conditions q_0 and $q_0 + \delta q$. Namely it is not necessary to hold the following relation;

$$\lim_{\delta q \to 0} \langle \phi_0(q) | \phi_0(q + \delta q) \rangle = 1. \tag{2.6}$$

When there holds the condition (2.6) for any value of q, the solution of the CHF equation $|\phi_0(q)\rangle$ in the $\{q\}$-space may just correspond to a single differentiable line in the $\{x_{\mu i}\}$-space. In this case, the configuration of $|\phi_0(q)\rangle$ changes smoothly with respect to q. When there does not hold the condition (2.6), two neighboring solutions $|\phi_0(q)\rangle$ and $|\phi_0(q + \delta q)\rangle$ belong to different CHF-lines with different configurations. This situation often happens because of the many-to-one transformation between the $\{x_{\mu i}\}$-space and $\{q\}$-space.

In actual numerical calculations in solving Eqs. (2.1) and (2.2), one has to use the discrete values for the constraining variables $\langle \hat{Q} \rangle = q_0, q_1, q_2, \cdots$. Thus one has to establish a practical method to get the continuous CHF-lines in the $\{q\}$-space, by keeping track to the differentiable CHF-lines in the $\{x_{\mu i}\}$-space.

Let us first discuss the continuity property of the single Slater-determinant in the $\{x_{\mu i}\}$-space. By means of Eqs. (2.3) and (2.4), the position of $|\phi\rangle$ in the TDHF coordinate system is expressed as $\{x_{\mu i}\}$. The distance between $|\phi\rangle$ and $|\phi_0\rangle$ is then given by the usual metric $\sum_{\mu i} x_{\mu i}^2$. On the other hand, the overlap between two single Slater-determinant is expressed as

$$\langle \phi_0 | \phi \rangle = \langle \phi_0 | e^{\hat{F}} | \phi_0 \rangle = \det |\langle \psi_j^{(0)} | \psi_i \rangle| = \det(\sqrt{I - C^\dagger C})_{ji} = \det(\sqrt{I - x^\dagger x/2})_{ji}, \tag{2.7}$$

where the single Slater-determinants $|\phi_0\rangle$ and $|\phi\rangle$ are described by the single-hole wave functions $\{\psi_j^{(0)}; j = 1, \cdots, N\}$ and $\{\psi_j; j = 1, \cdots, N\}$, respectively. From the above equation, it is clearly seen that the single Slater-determinant is a continuous function of $\{x_{\mu i}\}$ as well as an overlap between $|\phi\rangle$ and $|\phi_0\rangle$. In other words, the distance between $|\phi_0\rangle$ and $|\phi\rangle$ is measured by the overlap in Eq.(2.7). As is seen from

Eq.(2.7) and will be discussed in Sect. 3.2, it is possible to find the HF state $|\phi\rangle$ which lies at the nearest distance from a given single Slater-determinant $|\phi_0\rangle$ (which will be called a *reference state* (RS)) in the $\{x_{\mu i}\}$-space, by imposing the *maximum overlap criteria* (MOC, which will be discussed in Eq.(3.8)) with respect to the RS. Since this method provides us with the most nearest neighbor state for a given RS in the $\{x_{\mu i}\}$-space, it will be referred to a *RS-method.*

Secondly, we treat how to numerically get a *continuous CHF-lines* in the $\{q\}$-space by using a finite δq. Let $|\phi(q)\rangle$ be a known CHF state satisfying a given constrained condition $\langle\hat{Q}\rangle = q$, which is described by a set of single-particle wave functions $\{|\psi_i(q)\rangle; i = 1, \cdots, N\}$. In order to find an unknown CHF state $|\phi(q+\delta q)\rangle$ at $\langle\hat{Q}\rangle = q + \delta q$, which is continuously connected with $|\phi(q)\rangle$, we will use a condition given by

$$\lim_{\delta q \to 0} \langle\psi_i(q)|\psi_i(q+\delta q)\rangle = 1, \quad i = 1, \cdots, N, \tag{2.8}$$

which gives a more accurate condition than Eq.(2.6). Physically, the above condition means that the configuration specifying the single Slater-determinant on the CHF-line should change continuously, depending on the constraining variable q. In Sect.3.3, a new algorithm for numerically expressing the analytic condition (2.8) will be discussed by using the RS-method. When a resultant CHF-line does not depend on a choice of the small quantity δq, the analytic relation (2.8) is regarded to be satisfied numerically. Since the CHF solution at $q + \delta q$ is dictated by the configuration of the preceding CHF solution at q rather than by the minimum energy requirement, the above method will be called the *configuration dictated CHF method.*

At the end of this section, it should be noted that a symptom of the maximum overlap methods has been used phenomenologically near the single-particle level-crossing region [8, 10]. It intended to obtain a diabatic collective potential and a set of diabatic single-particle states by keeping the configuration of the single Slater-determinants unchanged.

3 Searching for Many High-Lying Hartree-Fock States

3.1 Constrained Hartree-Fock Calculation with Skyrme Force

Before explaining a new algorithm to exploit the continuity property of the CHF-lines, in this subsection, we outline the basic numerical method. To demonstrate an applicability of it, numerical calculation are carried out for $Z = 38$ and $N = 44$ (^{82}Sr) by using the Hamiltonian with the Skyrme force[12]. The used parameters are type SIII[13]. The major shell is included up to $N_0 = 8$. We assume the time reversal symmetry, the axial symmetry and reflection symmetry. The one-body Hamiltonian

is then block diagonal specified by the z-component of the angular momentum and the parity of the single-particle states Ω^π and each single particle level has two-fold degeneracy. Since the pairing correlations are not incorporated into the mean-field, in this paper, the nucleon number in each block gives an additional quantum number. We use the deformed harmonic oscillator base in cylindrical coordinate, which has two parameters, $\hbar\omega_r$ and $\hbar\omega_z$. The optimization of these parameters is performed for the HF ground state. These values are kept untouched in other calculations only for simplicity. The optimum choice for these parameters effectively takes into account the effects coming from the higher major shells $N_0 > 8$.

Instead of Eq.(2.1), we use the quadratic constraint [15] expressed as

$$\delta(\langle\hat{H}\rangle - \frac{c}{2}(\langle\hat{Q}_{20}\rangle - q_{\rm input})^2) = 0, \tag{3.1}$$

where $q_{\rm input}$ is a control parameter to vary the expectation value $\langle\hat{Q}_{20}\rangle$. In order to represent numerical results, we use the dimensionless deformation parameter $\tilde{\beta} = \langle\hat{Q}_{20}\rangle/\langle r^2\rangle$. The Lagrange multiplier λ is given by,

$$\lambda = c\,(\langle\hat{Q}_{20}\rangle - q_{\rm input}), \tag{3.2}$$

which has a sense even in the convergence process. Note that there holds $\langle\hat{Q}_{20}\rangle \neq q_{\rm input}$ except for the HF points. The parameter c defines a unit of $\delta q_{\rm input}$, and is chosen to be 1.0×10^{-4}[MeV/fm^4]. Any choice of this parameter does not affect on any physical quantity. The Hamiltonian represented for the single Slater-determinant $|\phi\rangle$ is given as;

$$\hat{H} - \lambda\hat{Q}_{20} = \langle\hat{H} - \lambda\hat{Q}_{20}\rangle + h[\rho]_{\alpha\beta} : c^\dagger_\alpha c_\beta : + : \hat{H} - \lambda\hat{Q}_{20} : \tag{3.3}$$

where $h[\rho]$ is the one-body Hamiltonian matrix depending on the density matrix $\rho_{\alpha\beta} = \langle\phi|c^\dagger_\beta c_\alpha|\phi\rangle$ and the symbol : : denotes the normal product with respect to $|\phi\rangle$.

To stabilize the convergence process, the one-body Hamiltonian to be diagonalized in the n-th iteration is defined by the following recursion formula

$$h^{(n)} = \begin{cases} h[\rho^{(0)}], & (n = 0) \\ (1-s)\,h^{(n-1)} + s\,h[\rho^{(n)}], & (n \geq 1) \end{cases} \tag{3.4}$$

where $\rho^{(n)}$ is the density matrix for the n-th step single Slater-determinant $|\phi^{(n)}\rangle$ in the convergence process reaching for $|\phi\rangle$. In our numerical calculation of using the Skyrme interaction, the above recursion formula is expressed in the coordinate space, and the convergent solutions are obtained by choosing s to be mainly within a range of $0.4 \sim 0.6$.

In order to get the CHF-lines, the accuracy of the single-particle wave function is the most important feature in our method. Our convergence condition is given by using a sum of the second order variances of the hole-state energies,

$$\log\Delta^{(n)} = \sum_{\{i\in\text{hole}\}} \log\Delta_i^{(n)}; \quad \Delta_i^{(n)} \equiv \left(\langle\epsilon_i^{(n)2}\rangle - \langle\epsilon_i^{(n)}\rangle^2\right), \tag{3.5}$$

where,

$$\langle \epsilon_i^{(n)} \rangle = \langle \psi_i^{(n)} | h^{(n)} | \psi_i^{(n)} \rangle, \quad \langle \epsilon_i^{(n)2} \rangle = \langle \psi_i^{(n)} | h^{(n)2} | \psi_i^{(n)} \rangle, \tag{3.6}$$

are diagonal components calculated by the single-particle wave functions before diagonalization. The numerical convergence is completed when there holds a relation,

$$\sqrt{\Delta^{(n)}} < \delta_0, \quad \text{and} \quad \log \Delta^{(n)} > \overline{\log \Delta^{(n)}}, \tag{3.7}$$

where δ_0 is a sufficient small number, and $\overline{\log \Delta^{(n)}} = \frac{1}{K} \sum_{k=1}^{K} \log \Delta^{(n-k)}$ denotes the averaged value for the last K-steps. The first relation is a necessary condition for self-consistency on the iterative diagonalization procedure and the second is a saturate condition in the convergence calculation. When the condition (3.7) is satisfied, one gets the converged single-particle wave functions. In our numerical calculation, δ_0 is chosen to be 5.0×10^{-6} [MeV] and $K = 10$.

3.2 High-Lying Hartree-Fock States

Before discussing a numerical method for obtaining the continuously-connected CHF-line in the $\{q\}$-space which keeps track to a certain differentiable line in the $\{x_{\mu i}\}$-space, we start with discussing how to obtain the HF solutions which are situated higher than the adiabatic solution $|\phi_0(q)\rangle$.

Let us take some single Slater-determinant which does not necessarily satisfy the HF condition. For example, we choose a certain single Slater-determinant $|\phi^{\rm RS}\rangle$, which is expressed by a simple many-particle many-hole state with respect to the HF state $|\phi_0\rangle$. Namely, the occupied states in $|\phi^{\rm RS}\rangle$ are not the first N-lowest single-particle states. This state has a well defined configuration with respect to $|\phi_0\rangle$, and will be called a reference state (RS). Let us consider the high-lying HF state which is located at the nearest distance from the RS in the $\{x_{\mu i}\}$-space. To obtain the self-consistent HF solution, we use the nonlinear eigenvalue equation. In the usual ACHF method, one introduces a new density matrix constructed by the first N-lowest eigenvectors in each iteration. However, this definition of the hole states is by no means unique. One may find the high-lying HF state $|\phi\rangle$ located very near to the RS, by ordering a complete set of single-particle states $\{|\psi_j\rangle\}$ obtained in the convergence process reaching to $|\phi\rangle$, in such a way that there hold the following "maximum overlap criteria (MOC)",

$$\langle \psi_i^{RS} | \psi_j \rangle \simeq \delta_{ij}, \quad (\text{for all } i, j) \tag{3.8}$$

where $|\psi_i^{RS}\rangle$ denotes the i-th single-particle state in the RS. This simple relation defines an one-to-one correspondence between two sets of the single-particle wave functions in each iterative process. Thus, the MOC (3.8) provides us with one definit way to specify $|\phi\rangle$ by *referring* to the RS. Requiring the above criteria in each convergence step, one may get the HF state which has maximum overlap to the RS. The resultant HF state $|\phi\rangle$ is located at a point nearest to the RS. The method of

using the MOC with respect to the RS in every convergence process will be called the *RS-method.*

The iterative process of our program to obtain the high-lying HF-points is itemized as follows; Assume that there is a HF state $|\phi_0\rangle$ (*e.g.* the HF ground state). As an example of the RS, we choose the single Slater-determinant expressed by a many-particle many-hole state with respect to $|\phi_0\rangle$, that is,

$$|\phi^{\rm RS}\rangle = |\phi_{ph}\rangle, \quad |\phi_{ph}\rangle = \prod_i (\hat{c}^\dagger_{p_i}\hat{c}_{h_i})|\phi_0\rangle. \tag{3.9}$$

1. Start the iterative process by choosing the RS $|\phi^{\rm RS}\rangle$ in Eq.(3.9) as an initial Slater-determinant $|\phi^{(n=0)}\rangle$.
2. Make the one-body Hamiltonian $h[\rho^{(n)}]$ by using $|\phi^{(n)}\rangle$. (Since we are interested in the HF points, $h[\rho^{(n)}]$ used in this subsection is defined in Eq.(3.3) without constraining term.) One gets a new set of single-particle wave functions $\{|\psi_i^{(n+1)}\rangle\}$, by diagonalizing $h^{(n)}$ in Eq.(3.4).
3. The i-th single-particle wave functions $|\psi_i^{(n+1)}\rangle$ (, with $i \leq N$) are *arranged and chosen* in such a way that there hold the following relations,
$$|\langle\psi_i^{\rm RS}|\psi_i^{(n+1)}\rangle|^2 > |\langle\psi_i^{\rm RS}|\psi_j^{(n+1)}\rangle|^2, \quad (\text{for all } j > i, \text{ with } i = 1, 2, \cdots, N), \tag{3.10}$$
which is derived from requirement (3.8). In this step, one requires $\langle\psi_i^{\rm RS}|\psi_i^{(n+1)}\rangle > 0$ to eliminate an extra phase factor. In this way, one gets N-kinds of single-particle wave functions to be used in constructing the single Slater-determinant $|\phi^{(n+1)}\rangle$.
4. To satisfy the self-consistency condition (3.7), the iteration from the step 2 to 3 should be repeated.

When the self-consistency condition is satisfied, one gets the high-lying HF state whose configuration is dictated by that of $|\phi^{\rm RS}\rangle$. In Fig.1, the convergence process to the high-lying HF state is illustrated. As is easily recognized from Fig.1b, the iteration is started from the proton 2p-2h state in the $(1/2)^-$-block; By using the asymptotic quantum numbers, it is expressed as $(\pi[310]1/2^-)^{-2}(\pi[301]1/2^-)^2$ with respect to the lowest prolate HF-point at $\tilde{\beta} \simeq 0.1$, which is denoted by $|\phi_0\rangle$ in Fig.2a. It is seen that the convergence in the total energy (Fig.1a) and the single-particle energies (Fig.1b) are accomplished much faster than the condition (3.7) in Fig.1c. With this very severe numerical self-consistency condition, the accuracy of each single-particle energy, $\sqrt{\Delta_i^{(n)}}$, is about 10^{-7} MeV, which is mainly coming from the accuracy of diagonalization routine. The convergence process from the 2p-2h state to the resultant HF state denoted by $|\phi_1\rangle$ is depicted in Fig.1d and Fig.2a.

It is easily recognized that the present numerical method is different from the adiabatic iterative diagonalization method only in the step 3, where the single-particle

wave functions are arranged not in order of the single-particle energy but in order of the overlap to the single-particle wave functions in the RS. This means that the conventional iterative diagonalization program is easily converted to the present one by a very small modification.

Zheng *et.al.*[14] got many-particle many-hole high-lying HF points. Since their one-body Hamiltonian is block diagonalized due to the assumed symmetry (parity, axial symmetry, etc.), the nucleon number in each block is regarded as an additional quantum number. In their calculation, they reached to the high-lying HF points which correspond to the most energetically favorable states under a given nucleon number distributed in each block. It should be emphasized that our present method reproduce not only their results, but also other many high-lying HF points which have a common nucleon number distributed in each block. The high-lying HF state $|\phi_1\rangle$ is just one example.

3.3 Local Configuration Dictated Method

Here it should be noticed that the RS-method discussed in the previous subsection has variety of applications. In this subsection, we treat how to numerically obtain the CHF-lines in the $\{q\}$-space.

Suppose there exists a self-consistent high-lying HF point $|\phi_1\rangle$ obtained by using the RS-method. By using an expectation value of the constraining operator $q_{10} = \langle\phi_1|\hat{Q}|\phi_1\rangle$, the state $|\phi_1\rangle$ is expressed as $|\phi^{\rm CHF}(q_{10})\rangle$. Namely, the state $|\phi^{\rm CHF}(q_{10})\rangle$ can also be regarded as a solution of the CHF equations (2.1) and (2.2) at a given value $\langle\hat{Q}\rangle = q_{10}$.

In solving the CHF equation for getting an adjacent CHF state continuously connected with $|\phi^{\rm CHF}(q_{10})\rangle$, one may apply the RS-method. In this case, one chooses $|\phi^{\rm CHF}(q_{10})\rangle$ as the RS, and sets $q_{\rm input} = q_{10} + \delta q_{\rm input}$ in Eq.(3.1). Here, $\delta q_{\rm input}$ is very small increment which will be discussed below. The resultant state obtained after convergence gives the CHF state $|\phi^{\rm CHF}(q_{11})\rangle$ where q_{11} is an expectation value of $\hat{Q}$. In obtaining the next adjacent CHF state continuously connected with $|\phi^{\rm CHF}(q_{11})\rangle$, one may repeat the same procedure by choosing $|\phi^{\rm CHF}(q_{11})\rangle$ as a new RS, and by setting $q_{\rm input} = q_{10} + 2\delta q_{\rm input}$. In this way, one gets the continuous CHF-line by starting from $|\phi_1\rangle$.

In this procedure, there still remains an important problem how to choose the magnitude of $\delta q_{\rm input}$ so as to meet the continuity condition given by Eq.(2.6) or Eq.(2.8). Since the relation between the $\{x_{\mu i}\}$- and $\{q\}$-spaces is given by the complex many-to-one transformation in Eq.(2.5), the continuity condition should be satisfied as rigorously as possible, and should be uniformly satisfied at any point on the line. For this aim, the magnitude of $\delta q_{\rm input}$ is treated as a variable quantity in our program.

Let $|\psi_i^{\rm RS}\rangle$ be the i-th single-particle occupied state in the known CHF state which is chosen as the RS, and let $|\psi_i^{(n)}\rangle$ be the i-th single-particle occupied state obtained in the n-th iteration to reach for the adjoining CHF solution. Here, $|\psi_i^{(n)}\rangle$ are arranged

by using the MOC in Eq.(3.10). As is easily understood, the adjoining CHF state is located at the nearest distance from the RS in the $\{x_{\mu i}\}$-space, and is also located at a point with small increment $\delta q_{\rm input}$ from the RS in the $\{q\}$-space. In order to find the adjacent CHF solution which is continuously connected with the RS, one start with solving the CHF equation by applying the RS-method, with the initial increment value $\delta q_{\rm input} = \delta q_{\rm max}$.

When one of the diagonal components of the overlap matrix between the single-particle wave functions in the n-th iteration and those in the RS does not satisfy a relation,

$$|\langle \psi_i^{\rm RS} | \psi_i^{(n)} \rangle|^2 \geq f_0, \tag{3.11}$$

where f_0 denotes an under limit of the overlap and is chosen to be mainly 0.9 in our calculation, one has to try again the same convergence process by making $\delta q_{\rm input}$ smaller. Namely, one has to find a CHF solution at a new point which is located much nearer to the RS than the previous trial. In our program, a new $\delta q_{\rm input}$ is introduced by multiplying a factor one half to the previous value. When one obtains two successive adjoining CHF points by applying the same increment, on the other hand, the increment $\delta q_{\rm input}$ to the subsequent point is twice enlarged from the previous value. In this case, we put a restriction that the $\delta q_{\rm input}$ should not exceed the initial value $\delta q_{\rm max}$.

By using the above procedure, the magnitude of $\delta q_{\rm input}$ is automatically adjusted in our program so that the relation (3.11) is satisfied at any point on the line. When the resultant line does not depend on a choice of f_0, our program works successfully to numerically find the CHF-line which satisfies the analytic relation (2.6). Here it should be noticed that the very severe self-consistency condition (3.7) imposed in our numerical calculation is also important in finding the CHF-lines.

In Fig.2a, the CHF-lines starting from $|\phi_0\rangle$ and $|\phi_1\rangle$ are illustrated. An employed value of the maximum increment is $\delta q_{\rm max} \simeq 20[{\rm fm}^2]$. The calculated points in the $\{q\}$-space automatically selected by our program are illustrated by open rhombuses. In Fig.2b, the overlap between two adjacent CHF solutions $|\langle \phi^{CHF}(q_i) | \phi^{CHF}(q_{i+1}) \rangle|^2$ along the CHF-line starting from $|\phi_0\rangle$ is shown. When one imposes $f_0 = 0.99$, it turns out that the resultant CHF-line is lying on the same line obtained under $f_0 = 0.9$ in Fig.2a. The overlap between the numerically obtained neighboring CHF states takes a value very near to 1, which is also illustrated in Fig.2b. Since the resultant CHF-line does not depend on the value of f_0, our program can follow the continuous CHF-line which satisfies the analytic condition (2.8), and the value $f_0 = 0.9$ already gives a sufficient accuracy to numerically guarantee the relation (2.6). The present numerical method will be called the *local configuration dictated* (LCD-) method, because it applies the RS-method by introducing a new RS at each discretized point.

4 Searching for Other Continuous CHF-line

LCD-method discussed in the previous subsection is very useful in getting the
F-line, when one knows the high-lying HF point in advance. In this subsection,
discuss how to find other CHF point which lies on an unknown CHF-line in the
space. If one gets such CHF point, one may obtain a new CHF-line by using the
)-method.

Suppose there are two differentiable CHF-lines in the $\{x_{\mu i}\}$-space denoted by A
B. When these lines are closely located in the $\{x_{\mu i}\}$-space, the overlap between
$q_\alpha)\rangle$ at some point on the line A, and $|\phi^B(q_\beta)\rangle$ at another point on the line B
a chance to become larger than that between two points on the same line A;

$$|\langle\phi^A(q_\alpha)|\phi^B(q_\beta)\rangle|^2 > |\langle\phi^A(q_\alpha)|\phi^A(q_\beta)\rangle|^2. \tag{3.12}$$

, q_α and q_β in the parentheses are the expectation values of the constraining
ator $\hat{Q}$ for each CHF state. In this case, the CHF solution by using the RS-
iod where $|\phi^A(q_\alpha)\rangle$ is chosen as the RS with the constrained condition $\langle\hat{Q}\rangle = q_\beta$,
the state $|\phi^B(q_\beta)\rangle$ rather than $|\phi^A(q_\beta)\rangle$.

Following the above scenario, one employs the RS-method where any state on the
vn CHF-line is chosen as the RS. Suppose the single Slater-determinant $|\phi^A(q_\alpha)\rangle$
esses a state on the known CHF-line A. To get an adjacent CHF state, one applies
RS-method by choosing $|\phi^A(q_\alpha)\rangle$ as the RS, and by setting $q_{\rm input} = q^{(\alpha)} + \delta q_{\rm input}$.
$q^{(\alpha)}$ denotes an input value in Eq.(3.1) to be used in obtaining the CHF solution
$_\alpha)\rangle$. In this procedure, the magnitude $\delta q_{\rm input}$ is chosen to be much larger than
used in the LCD-method. Furthermore, the step $\delta q_{\rm input}$ in this procedure is kept
ant, and the condition (3.11) is not imposed, unlike the case in the LCD-method
ssed in the previous subsection.

he resultant state obtained after convergence gives the CHF state $|\phi^A(q_1)\rangle$, where
the expectation value of $\hat{Q}$ with respect to the resultant convergent solution.
et the n-th adjacent CHF state from $q^{(\alpha)}$, one applies the RS-method by using
ame RS as before, *i.e.*, $|\phi^A(q_\alpha)\rangle$, with $q_{\rm input} = q^{(\alpha)} + n\delta q_{\rm input}$. In this way, one
a set of CHF states $\{|\phi^A(q_1)\rangle, |\phi^A(q_2)\rangle, \cdots\}$ whose structure are dictated by the
RS, $|\phi^A(q_\alpha)\rangle$. A first few CHF states obtained by this method rest on line A.
a few steps later, one may have a chance to obtain a CHF state which rests
e other line B. Since the present method does not require the condition (2.6),
ondition (3.11), it has a chance to jump over from one CHF-line to the other.
is sense, the above method is considered to be one possible realization of the
guration (C-)CHF method proposed in ref.[4].

order to demonstrate an applicability of the present method, we choose the
t prolate HF state $|\phi_0\rangle$ at $\tilde{\beta} \simeq 0.1$ on the known CHF-line A as the fixed RS.
pplying $\delta q_{\rm input} = 115$ [fm^2], we get a set of CHF states $\{|\phi^A(q_1)\rangle, |\phi^A(q_2)\rangle, \cdots\}$
rated by open rhombuses in Fig.3a. From this figure, it is clearly seen that
resent method gives a practical way to find another CHF-line denoted by B.

Actually, the line B is obtained by applying the LCD-method discussed in the previous subsection, after having gotten the CHF points denoted by open rhombuses on the line B.

The self-consistent single-particle energies on the set of CHF points are shown in Fig.3b. The occupied states are expressed by the black circles, while the unoccupied states by the open circles. Remember that the single-particle wave functions in each iterative process for reaching these CHF points are arranged and chosen by using the relation (3.10) with respect to the fixed RS, $|\phi_0\rangle$. Consequently, one can establish an one-to-one correspondence between the single-particle states in these CHF points and those in $|\phi_0\rangle$. With the aid of this one-to-one correspondence, the black and open circles are connected by the solid lines.

In Fig.3b, the single-particle energies on the line A are indicated by the dashed lines. Note that the single-particle energies of the set of CHF states $\{|\phi^A(q_1)\rangle, |\phi^A(q_2)\rangle, \cdots\}$ before the jumping are on the dashed lines. As is recognized from Fig.3b, the rearrangement of the configuration takes place at the region where the jumping from the line A to line B happens. However, one should be careful in using the words "configuration change". When one use this words *locally*, there does not occur any rearrangement in the configuration either along the line A nor along the line B, whereas the jumping from the line A to line B is associated with a configuration change, *i.e.* the occupied and the unoccupied states interchange their roles. On the other hand, the jumping from the line A to line B is *not* associated with a configuration change, when one discuss about the configuration of the state $|\phi_0\rangle$ *globally*. In other words, the set of CHF points $\{|\phi^A(q_1)\rangle, |\phi^A(q_2)\rangle, \cdots\}$ are always lying at the nearest distance from the fixed RS $|\phi_0\rangle$ in the $\{x_{\mu i}\}$-space, under a given distance $q_{\rm input} = q^{(\alpha)} + n\delta q_{\rm input}$ in the $\{q\}$-space.

Actually, the LCD-method discussed in the previous subsection emploies the RS-method dictated by the *local* configuration, whereas the method in this subsection uses the RS-method which is *globally* dictated by the fixed configuration of the RS, *i.e.* $|\phi_0\rangle$. Thus the method developed here will be called the *global configuration dictated* (GCD-) method.

4 Summary and Discussion

By using various applications of the RS-method stated in the previous section, we obtain many CHF-lines and many high-lying HF states which are shown in Fig.4a. Since a limited number of many-particle many-hole states in Eq.(3.9) are used as the RS in finding out the high-lying HF points in the present calculation, there certainly exist many other CHF-lines which are not shown in Fig. 4a. In obtaining many high-lying HF points, it turned out to be more efficient to choose the many-particle many-hole states built on various local *minima* as the RS, rather than to choose only those built on the HF ground state. When one applies the conventional ACHF, one gets a part of an envelop of the CHF-lines. In our numerical calculation, we

first apply the ACHF and get some HF points which are lying on the envelop. The ACHF calculation does not converge near the "band crossing" points where two CHF-lines degenerate accidentally. It only has a convergent solution when there are well separated local minima. Some other HF points are found by specifying the number of nucleons distributed in each Ω^{π}-block. The many-particle many-hole states are then constructed by using these HF points.

In Fig. 4b, the value of Lagrange multiplier λ is shown. Since λ is not single-valued function of deformation, it is desirable to use the quadratic constraint formalism. In our numerical calculation, it often happens that the high-lying HF point satisfying $\lambda = 0$ locates at a point slightly different from the local minimum. This is because of our simplified calculation where we use the fixed parameters of the deformed harmonic oscillator base $\hbar\omega_r$ and $\hbar\omega_z$ optimized for the ground state HF point. This discrepancy can be removed by optimizing the base parameters for each high-lying HF point. There are a few cases where the iteration for getting CHF-line does not converge. To make it converge, it may be one possible way to take larger values for f_0 in Eq.(3.11) so as to make δq smaller.

In the present paper, we have developed a new algorithm for getting many high-lying HF points. This method exploits the following property of the CHF equation within the TDHF-coordinate space $\{x_{\mu i}\}$; it gives continuous differentiable lines, and each HF point is located at one of these lines. In order to establish the numerical method, it is crucial to use the RS-method. It can find a solution of the HF variational equation (with and without constrained conditions), which lies at the nearest distance from an arbitrarily chosen RS in the $\{x_{\mu i}\}$-space. As is shown in this paper, this RS method is very simple and powerful, and clearly overcome an essential difficulty related to the adiabatic requirement. By applying it to the realistic case, its feasibility is demonstrated. In order to compare our numerical results with the experimental data, one has to include the pairing correlations as well as the effects of stationary rotation. This extension is straightforward and is now in progress.

In this paper, the structure of the $\{x_{\mu i}\}$-space are not explicitly discussed, because it is our present aim to get the high-lying HF points by going one step further from the conventional numerical method. Here, it is noticed that the various curves in Fig.4a should not be considered as the PES, except for a region very near to the local minimum points. Since these curves express the projection of the PES in the $\{x_{\mu i}\}$-space onto the $\{q\}$-space, we use the CHF-lines as a searching path to find out the high-lying HF sates. An dynamical relation between various HF points can only be explored within the TDHF-manifold. An extension to the dynamical problem of calculating the TDHF-trajectory is also in progress.

References

[1] J. L. Woods, K. Heyde, W. Nazarewicz, M. Huyse and P. van Duppen, Phys. Rep. 215, Nos. 3 & 4 (1992) 101

[2] W. Nazarewicz, Nucl. Phys. A557 (1993) 489c

[3] R. Bengtsson and W. Nazarewicz, Z. Phys. A 334 (1989), 269

[4] K. Iwasawa, F. Sakata, W. Nazarewicz, T. Marumori and J. Terasaki, INS-Rep.-1036, (June, 1994) submitted to Phys. Lett.B

[5] F. Sakata, in preparation.

[6] J. L. Egido, H.-J. Mang and P. Ring, Nucl. Phys. A334 (1980) 1

[7] I. Hamamoto, Nucl. Phys. A271 (1976) 15

[8] A. Lukasiak, W. Cassing and W. Nörenberg, Nucl. Phys. A426 (1984) 181

[9] Y. R. Shimizu and K. Matsuyanagi, Prog. Theor. Phys. 74 (1985) 1346

[10] T. Bengtsson, Nucl. Phys. A496 (1989) 56

[11] J. Terasaki, F. Sakata and K. Iwasawa, INS-Rep.-1046 (Aug. 1994)

[12] D. Vautherin and D. M. Brink, Phys. Rev. C5 (1972) 626
D. Vautherin, Phys. Rev. C7 (1973) 296
J. Damgaard, H. C. Pauli, V. V. Pashkevich and V. M. Strutinsky, Nucl. Phys. A135 (1969) 432
M. Matsuo, private communication (1989)

[13] M. Beiner, H. Flocard, Nguen Van Giai and P. Quentin, Nucl. Phys. A238 (1985) 29

[14] D. C. Zheng, D. Berdichevsky and L. Zamik, Phys. Rev. C38 (1988) 437
D. C. Zheng, L. Zamik and D. Berdichevsky, Phys. Rev. C42 (1990) 1004

[15] H. Flocard, P. Quentin, A. K. Kerman and D. Vautherin, Nucl. Phys. A203 (1973) 433

Figure Captions:

Figure 1. Convergence process to the high-lying HF point started from the 2p-2h state with respect to $|\phi_0\rangle$. a) Convergence of the total energy. Energy relative to $|\phi_0\rangle$ is expressed. b) Convergence of the single-particle energies. They are labeled by the asymptotic quantum numbers. Those having the same asymptotic quantum numbers are connected by the solid line. The black and open circles represent the occupied and unoccupied states, respectively. c) Convergence of the variance $(\Delta^{(n)})^{1/A}$ defined in Eq.(3.4). The single-particle wave functions are converged after 80 iterations. d) Convergence process to the high-lying HF point $|\phi_1\rangle$ started from the 2p-2h state $|\phi_{2p2h}\rangle$. Rearrangement of the mean-field due to the 2p-2h excitation is illustrated.

Figure 2. Continuous CHF-lines. The control parameter is $f_0 = 0.9$. a) The lower and upper lines are started from the HF points $|\phi_0\rangle$ and $|\phi_1\rangle$, respectively. The calculated points automatically selected by the program are shown by open rhombuses. b) The overlap between two adjacent single Slater-determinants at automatically selected points. For comparison, the case with $f_0 = 0.99$ is also shown.

Figure 3. New CHF points lying on an unknown CHF-line B. a) A set of CHF points on the line B are obtained by starting from $|\phi_0\rangle$ on the line A. In this calculation, the HF point $|\phi_0\rangle$ is always chosen as the RS and an increment $\delta q_{input} = 115$ [fm^2] is adopted. The CHF points obtained by the GCD-method are denoted by the open rhombuses. Solid curves giving the continuous CHF-lines are calculated by using the LCD-method in Sect.3.3. b) Self-consistent single-particle energies. Those calculated on the line A are expressed by the dashed lines. Those calculated at the CHF points obtained by the GCD-method are connected by the solid lines owing to the one-to-one correspondence by the MOC. The black and open circles on the solid lines represent the occupied and unoccupied states, respectively.

Figure 4. a) Many continuous CHF-lines and many high-lying HF points. b) Lagrange multipliers on various continuous CHF-lines.

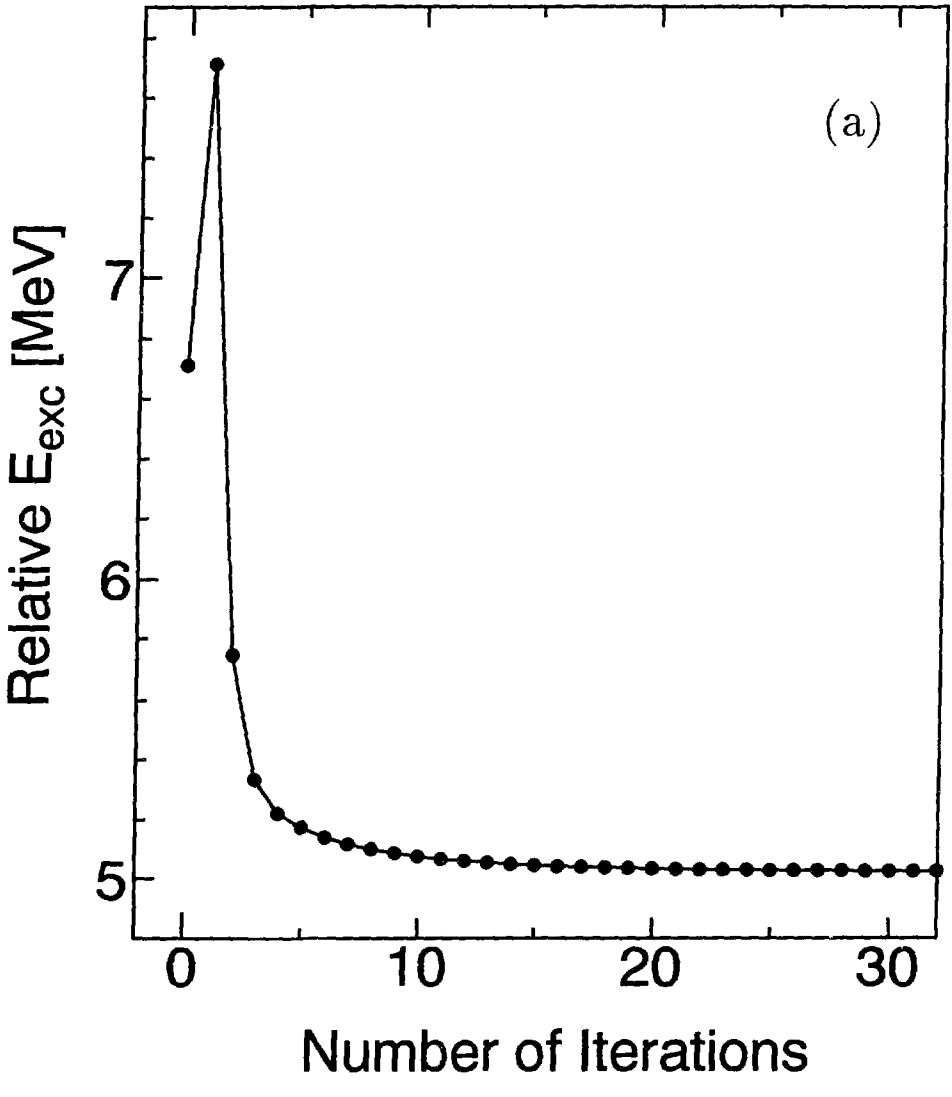

Fig.1 (a)

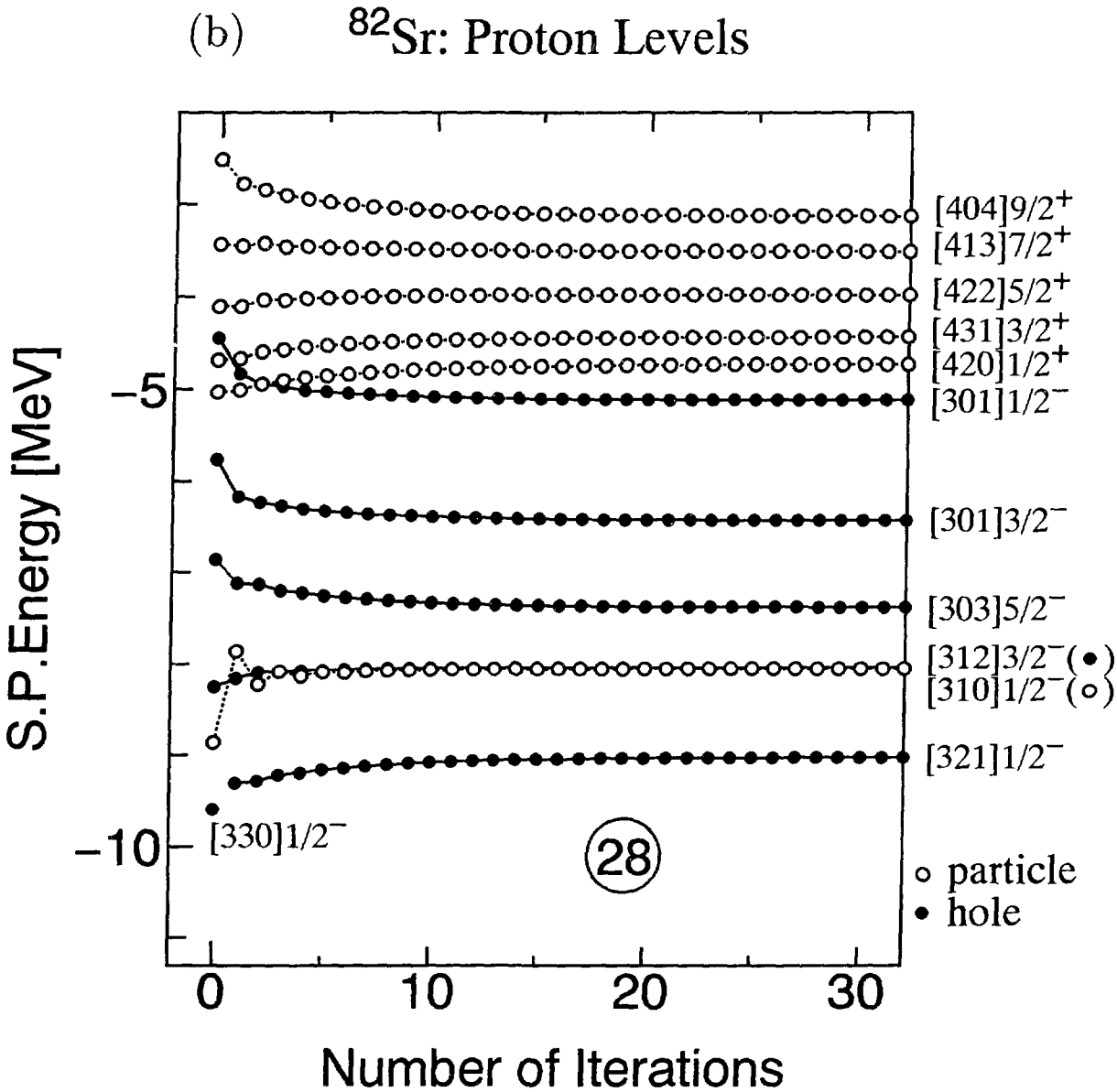
(b) ^{82}Sr: Proton Levels
S.P.Energy [MeV]
−5
−10
0
10
20
30
Number of Iterations
[404]9/2+
[413]7/2+
[422]5/2+
[431]3/2+
[420]1/2+
[301]1/2−
[301]3/2−
[303]5/2−
[312]3/2−(•)
[310]1/2−(○)
[321]1/2−
[330]1/2−
28
○ particle
• hole

Fig.1 (b)

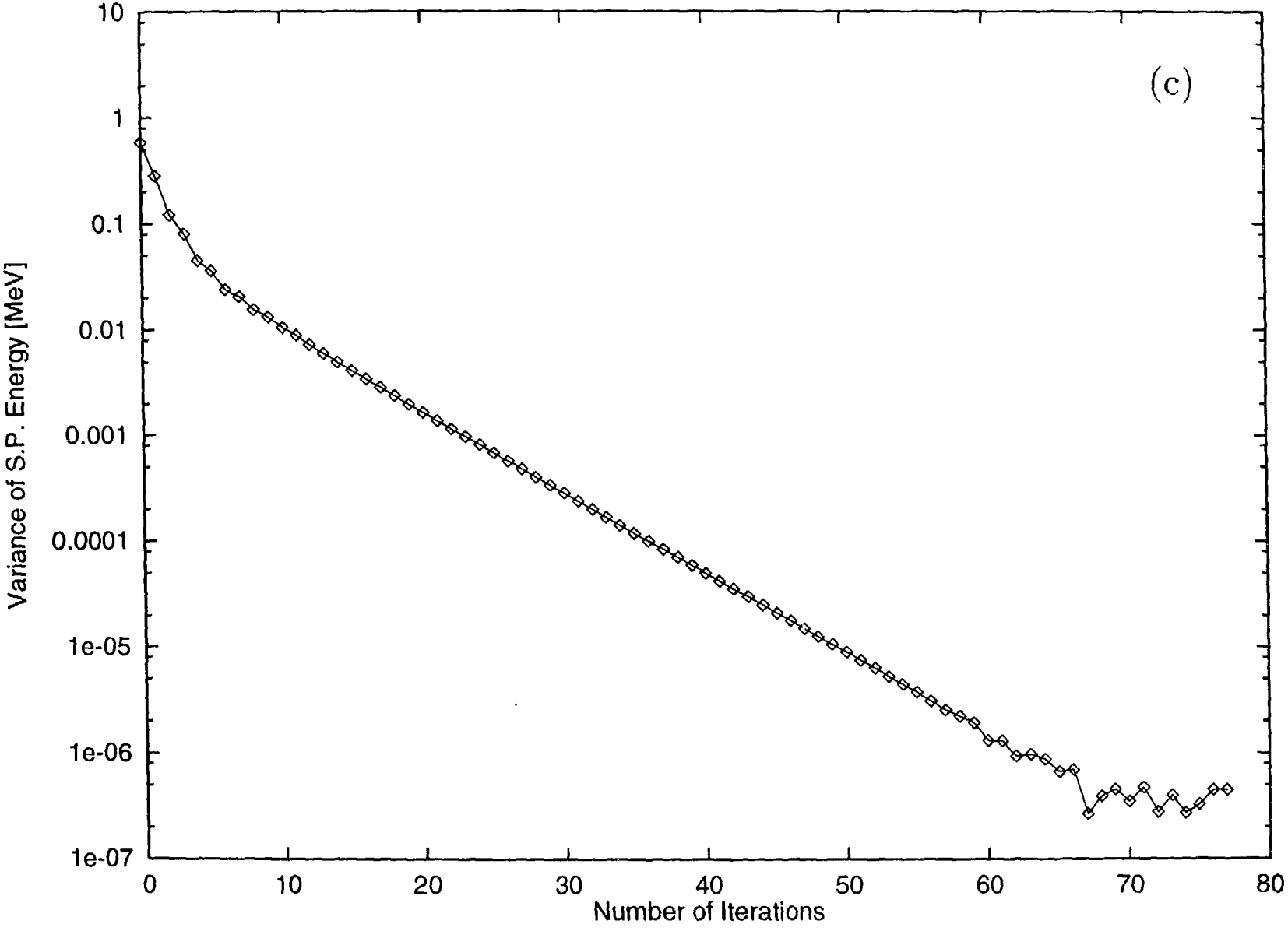
(c)
Variance of S.P. Energy [MeV]
10
1
0.1
0.01
0.001
0.0001
1e-05
1e-06
1e-07
0
10
20
30
40
50
60
70
80
Number of Iterations

Fig.1 (c)

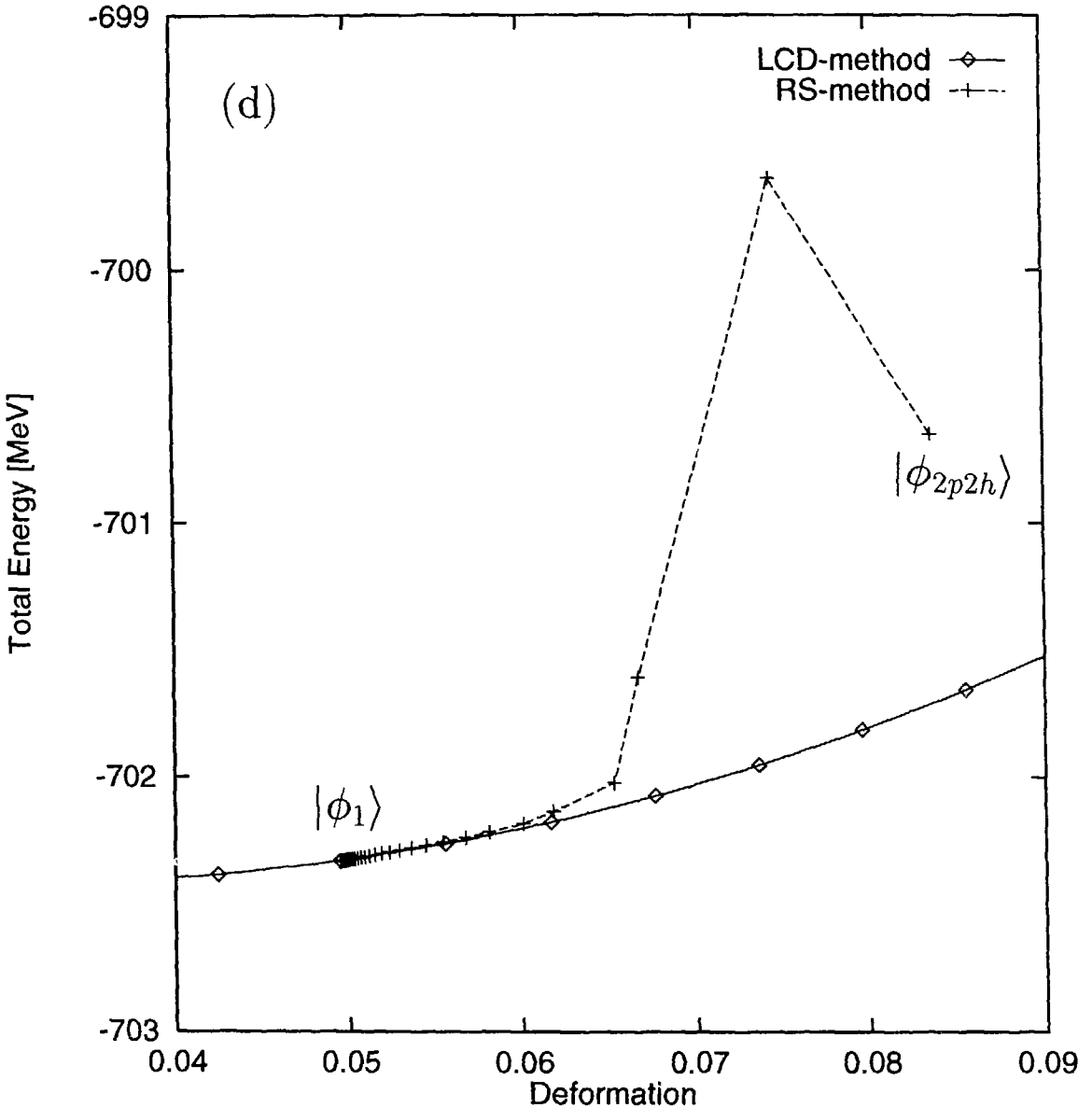
(d)
LCD-method
RS-method
$|\phi_{2p2h}\rangle$
$|\phi_1\rangle$
Total Energy [MeV]
-699
-700
-701
-702
-703
0.04
0.05
0.06
0.07
0.08
0.09
Deformation

Fig.1 (d)

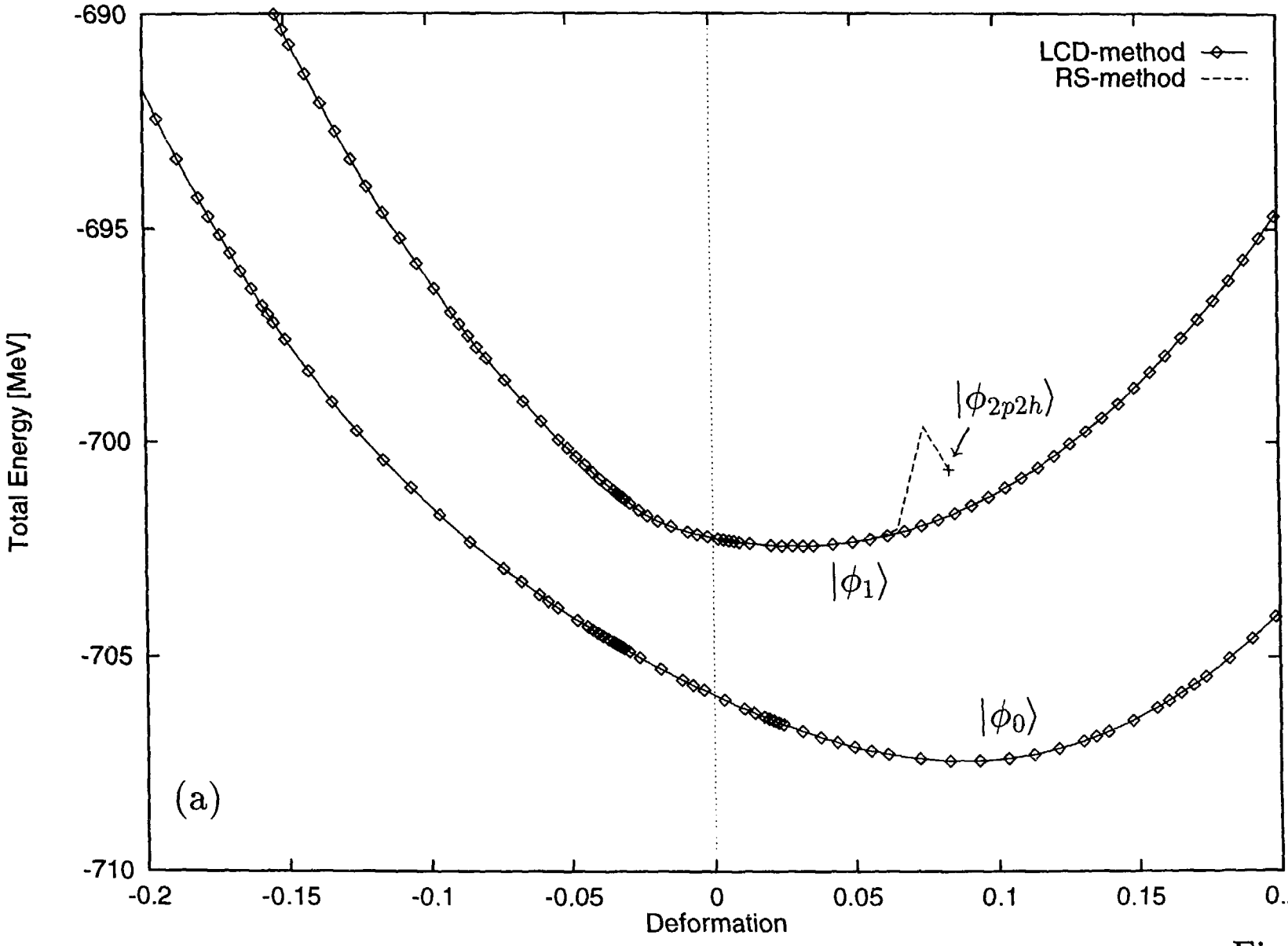
LCD-method
RS-method
$|\phi_{2p2h}\rangle$
$|\phi_1\rangle$
$|\phi_0\rangle$
(a)
Total Energy [MeV]
Deformation
-690
-695
-700
-705
-710
-0.2
-0.15
-0.1
-0.05
0
0.05
0.1
0.15
0.2

Fig.2 (a)

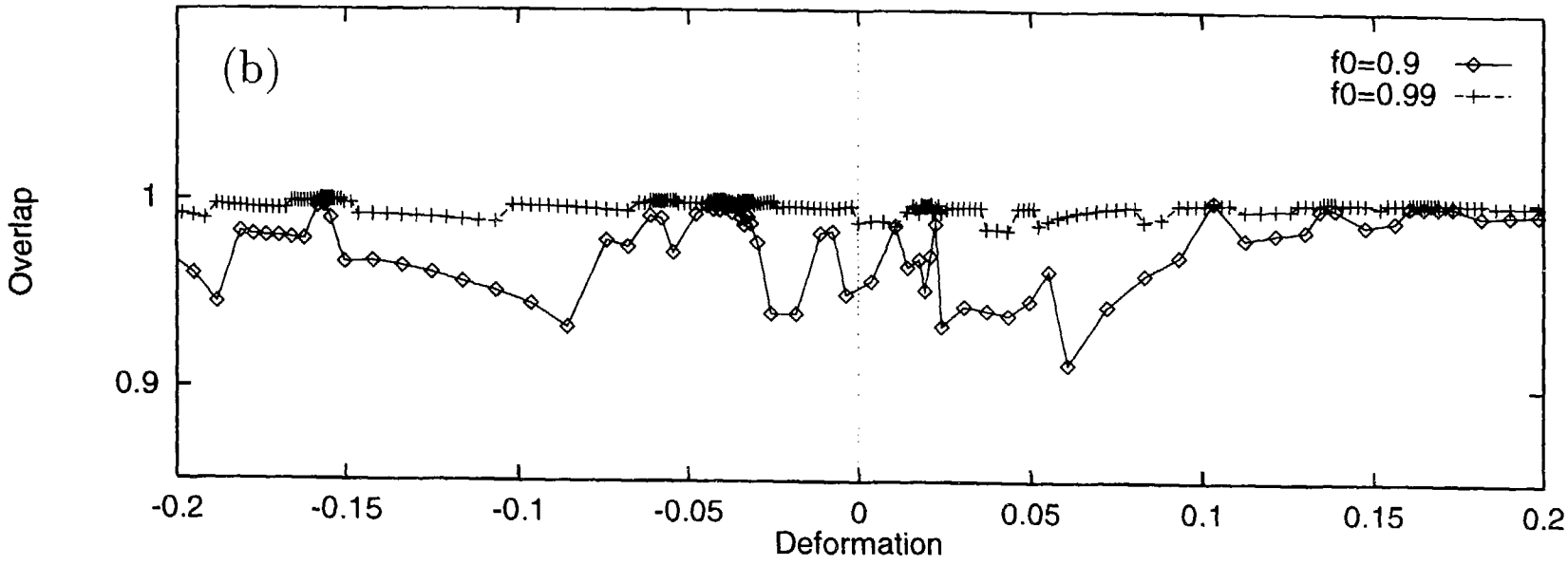
(b)
f0=0.9
f0=0.99
Overlap
1
0.9
-0.2
-0.15
-0.1
-0.05
0
0.05
0.1
0.15
0.2
Deformation

Fig.2 (b)

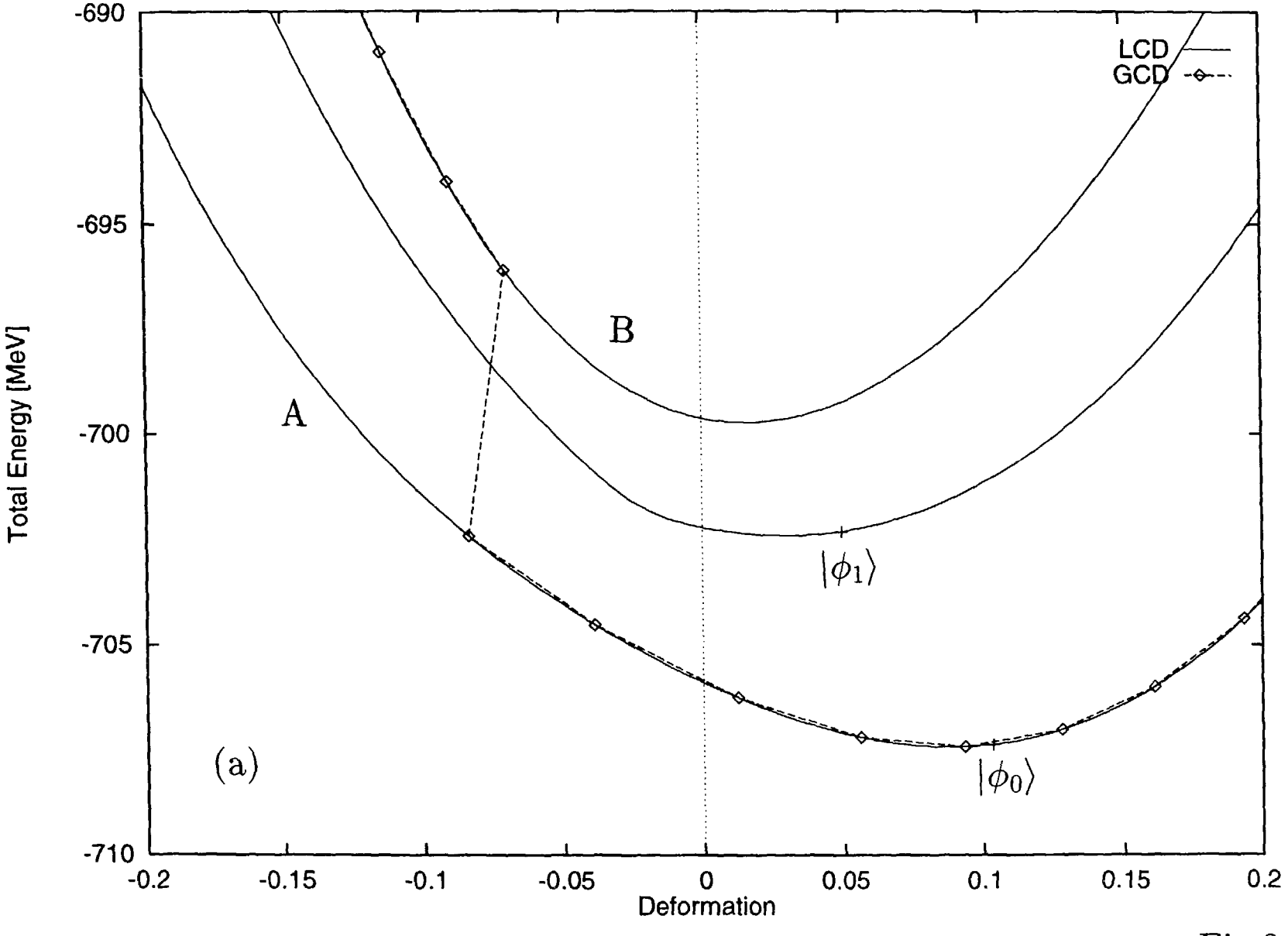
LCD
GCD
A
B
$|\phi_1\rangle$
$|\phi_0\rangle$
(a)
Total Energy [MeV]
Deformation
-690
-695
-700
-705
-710
-0.2
-0.15
-0.1
-0.05
0
0.05
0.1
0.15
0.2

Fig.3 (a)

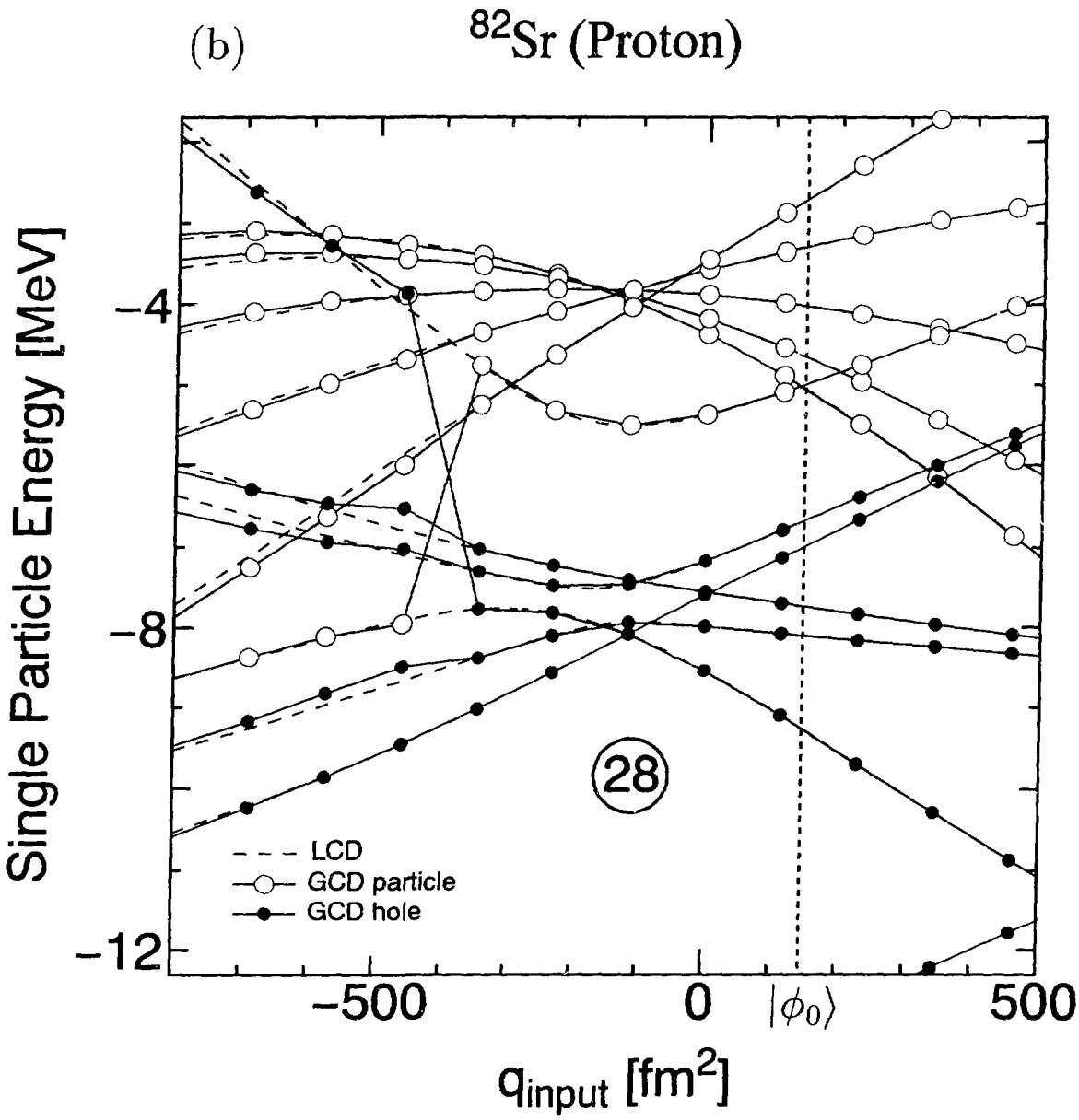
(b)
^{82}Sr (Proton)
Single Particle Energy [MeV]
-4
-8
-12
-500
0
$|\phi_0\rangle$
500
q_{input} [fm^2]
28
LCD
GCD particle
GCD hole

Fig.3 (b)

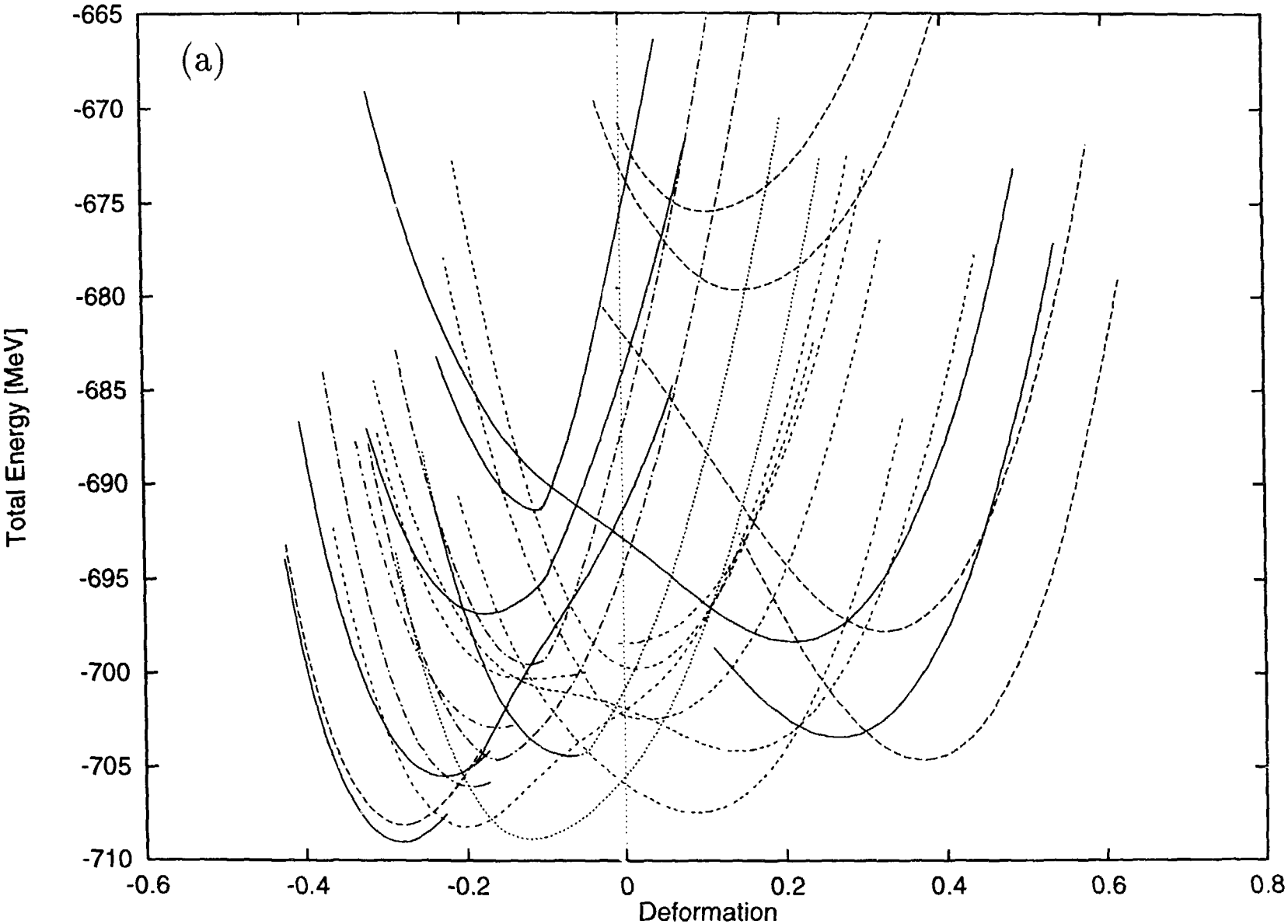
(a)
-665
-670
-675
-680
-685
-690
-695
-700
-705
-710
Total Energy [MeV]
-0.6
-0.4
-0.2
0
0.2
0.4
0.6
0.8
Deformation

Fig.4 (a)

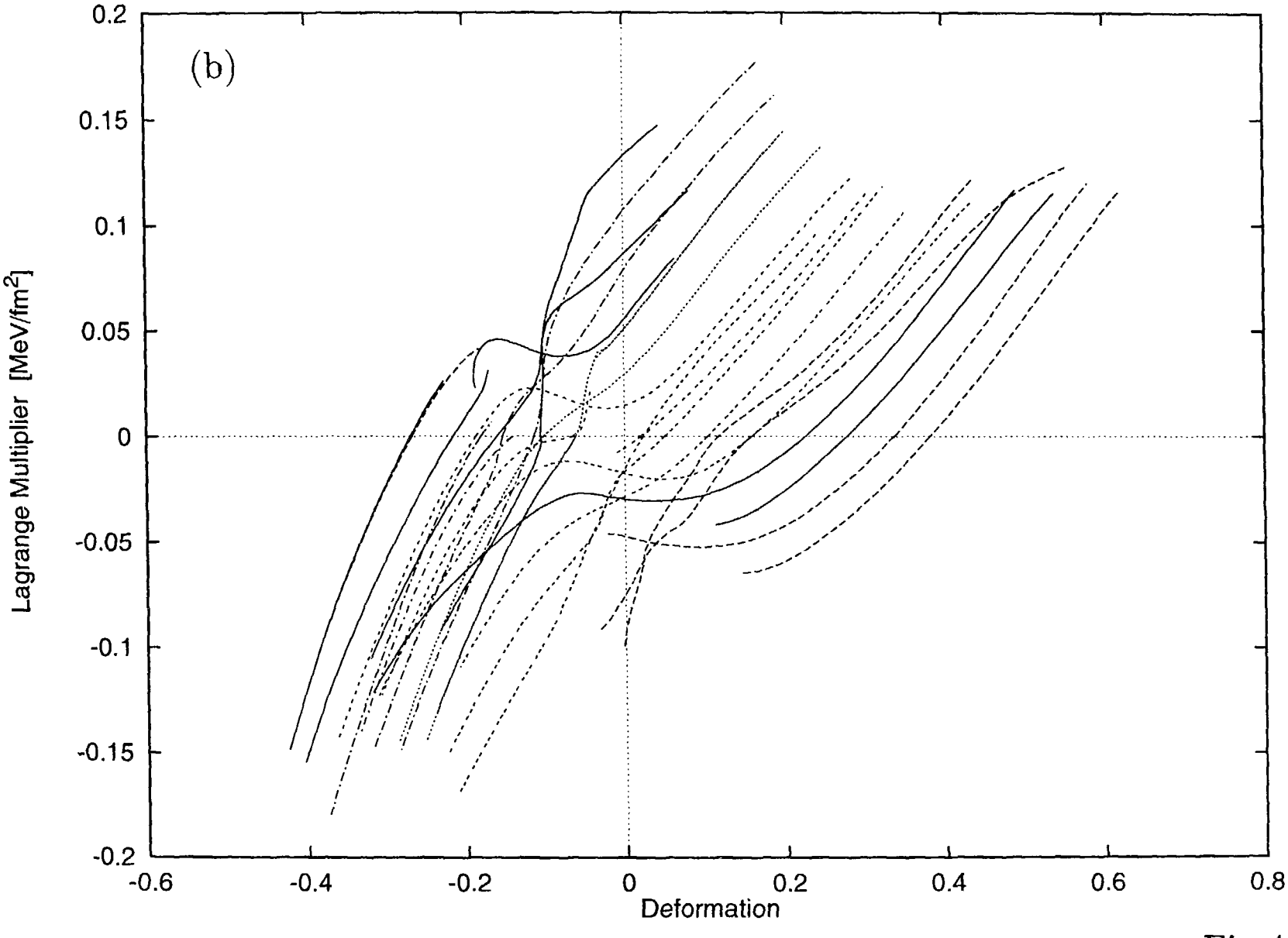
(b)
0.2
0.15
0.1
0.05
0
-0.05
-0.1
-0.15
-0.2
-0.6
-0.4
-0.2
0
0.2
0.4
0.6
0.8
Deformation
Lagrange Multiplier [MeV/fm^2]

Fig.4 (b)